INTERNATIONAL JOURNAL OF ENERGY RESEARCH
Int. J. Energy Res. 2002; **26**:93–104 (DOI: 10.1002/er.768)

A 3D Lagrangian particle model for the atmospheric dispersion of toxic pollutants

S. Raza[1,2], R. Avila[1,2,*,†] and J. Cervantes[2]

[1] *Instituto Nacional de Investigaciones Nucleares (ININ), Apdo. Postal 18-1027, México DF 11801, Mexico*
[2] *Facultad de Ingeniería, UNAM, México DF 04510, Mexico*

SUMMARY

A 3D Lagrangian particle model has been presented for the atmospheric dispersion of the toxic pollutants released from industrial stacks. As the mean wind speed and direction is changed with height in a real atmosphere, the height of the exhaust stack may have a strong impact on the pollutant dispersion and ground concentrations.

An elevated continuous release of non-buoyant gas in a neutrally stratified atmosphere has been simulated, for various stack heights. The turbulent atmospheric parameters like vertical profiles of fluctuating wind velocity components and eddy lifetime were calculated using a semi-empirical mathematical model.

The numerically calculated horizontal and vertical dispersion coefficients (σ_y and σ_z) are compared with the Pasquill's empirical σ's. The ground concentration as a function of downwind distance has been compared with the Green glow data. The ground concentrations for various release heights were compared with the Gaussian plume model. The comparison indicated a need for using either a modified Gaussian model or a 3D numerical mathematical model for pollutant dispersion and ground concentration calculations. Copyright © 2002 John Wiley & Sons, Ltd.

KEY WORDS: atmospheric dispersion; flow modelling; complex topography; numerical modelling; Lagrangian model; trajectory model

1. INTRODUCTION

When a gaseous effluent from an industrial stack is released to the atmosphere, it is transported and dispersed as a result of the mean and the fluctuating wind field. As a result the released plume is spread in the horizontal and vertical dimensions. The plume spread is normally expressed in terms of the dispersion coefficients σ_y (for the horizontal crosswind direction) and σ_z (for the

* Correspondence to: R. Avila, Departamento de Fisica, Instituto Nacional de Investigaciones Nucleares (ININ), Apartado Postal 18-1027, Col. Escandon, Mexico DF 11801, Mexico.
† E-mail: rar@nuclear.inin.mx

Contract/grant sponsor: Visualization Laboratory (DGSCA-UNAM) Mexico; Contract/grant sponsor: Consejo Nacional de Ciencia y Tecnologia; contract/grant number: 3328P-A; Contract/grant sponsor: Direction General de Apoyoal personal Académico-UNAM; contract/grant number: PAPITT No. IN105798.

Received 22 September 2000
Accepted 16 January 2001

Copyright © 2002 John Wiley & Sons, Ltd.

vertical direction). Empirical functions of these coefficients as a function of atmospheric stability class and downwind distance have been constructed and published for distances upto 100 km. The most commonly used are the Pasquill–Gifford (P–G) σ curves (Turner, 1994), which were derived from the Prairie Grass field data (Haugen, 1959). These σ's are applicable to rural conditions (with a roughness height $z_0 = 3$ cm) for near surface releases and are independent of the release height. The use of these σ's in the atmospheric dispersion applications has been the centre of continual arguments due to their role in regulatory measures. According to Hanna (1982) these curves were subjected to much misapplications to distances, sampling time and roughness outside of their range of derivation, leading to poor agreement with the observations. The confidence level for the P–G σ's is reduced for distances greater than 1 km, whereas, for the extreme conditions (highly unstable, A and highly stable, F) the confidence is reduced just after 500 m downwind (Hanna, 1984).

These dispersion coefficients (σ's), as mentioned before, provide a measure of the lateral and vertical standard deviations of the concentration distribution and account for the plume dimensions in the Gaussian plume model (GPM). This model has been widely used for industrial applications and its results are generally considered to be reliable within a factor of 2–4, for short distances (Turner, 1994). However, when the terrain conditions are complex such as mountains, lake or a seashore site, the reliability factor is much poor (Miller and Hively, 1987).

Owing to an increasing concern about environmental pollution, the atmospheric dispersion modelling has gained great interest in the recent years (Turner, 1997; Perdikaris and Mayinger, 1995). We, in this work, present the use of a 3D Lagrangian particle model (Avila, 1997), for the pollutant dispersion calculations for complex meteorological and terrain conditions. For the concentration calculations a puff-particle approach has been used (de Haan and Rotach, 1995).

2. COMPUTATIONAL METHODOLOGY

2.1. Windfield model

The model equations to calculate the 3D wind field components like vertical profiles of the mean wind, friction velocity, turbulent velocity fluctuations and the eddy lifetime are presented in this section. The mean wind profiles (see Figures 1 and 2) were obtained from the solution of a homogeneous planetary boundary layer model (Avila, 1997), which compared well with the observations taken over Leipzig city (Lettau, 1962).

The other turbulent wind parameters like velocity fluctuations and eddy lifetime were calculated using a semi-empirical mathematical model (Davis, 1983). The velocity fluctuations for the horizontal and vertical directions were calculated by generating a random number with normal distribution having the standard deviations given by the following relations:

$$(\overline{u'^2})^{1/2} = (\overline{v'^2})^{1/2} = \sigma_u(z) = \frac{2.2u_*(z)}{(1 + 15z/h)^{1/3}} \tag{1}$$

$$(\overline{w'^2})^{1/2} = \sigma_v(z) = 1.3u_*(z) \tag{2}$$

Copyright © 2002 John Wiley & Sons, Ltd.

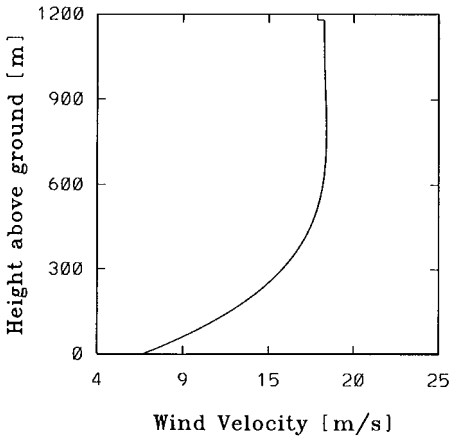

Figure 1. Vertical profile of the mean wind for a neutral atmosphere.

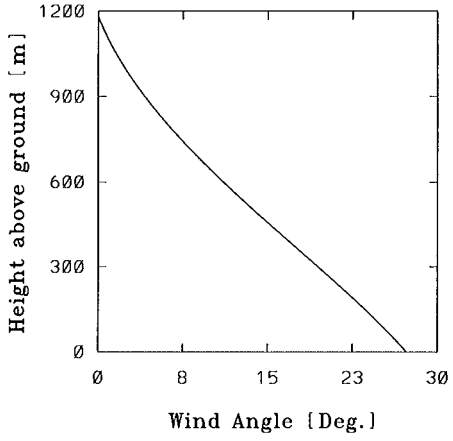

Figure 2. Vertical profile of the wind angle with the geostrophic wind, for a neutral atmosphere.

The vertical profiles calculated using the above equations have been presented in Figures 3 and 4. It may be observed that the velocity fluctuations/turbulence intensity is reduced with height.

The eddy lifetime (the duration for which these velocity fluctuations persist in the atmosphere) was calculated using the relation below:

$$T_{lw} = \frac{0.4z}{u_{0*}} \left(\frac{1}{(1 + 40\hat{z})} \right) \tag{3}$$

The vertical profile for the eddy lifetime is given in Figure 5. We observe that the eddy lifetime increases asymptotically, within the boundary layer and has a max value of about 100 s outside

Copyright © 2002 John Wiley & Sons, Ltd.

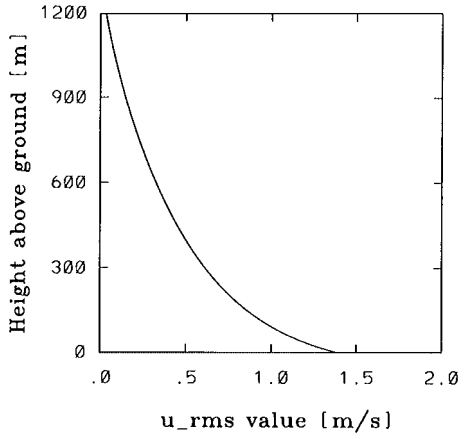

Figure 3. Horizontal velocity fluctuation profiles for a neutral atmosphere.

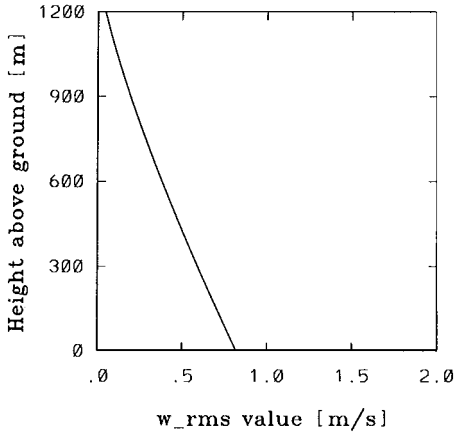

Figure 4. Vertical velocity fluctuation profiles for a neutral atmosphere.

the PBL (Davis, 1983). This eddy profile compared well (not presented here) with that calculated by the relation (Avila, 1997):

$$T_l = C_T \frac{\kappa}{\varepsilon} \tag{4}$$

where κ is the turbulent kinetic energy, ε is the energy dissipation rate and C_T is an empirical factor having value 0.3.

2.2. Particle dispersion model

A fully 3D Lagrangian Particle trajectory Model (LPM) for the atmospheric dispersion of industrial pollutants is presented. The model has been applied to a non-buoyant toxic gas release

Copyright © 2002 John Wiley & Sons, Ltd.

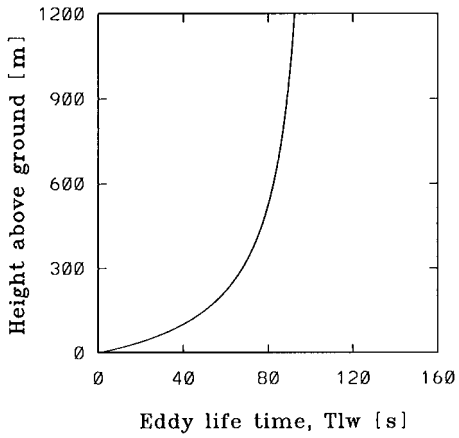

Figure 5. Eddy lifetime for a neutral atmosphere.

from an industrial exhaust stack. A discrete-time step Monte Carlo process (or 'jump model') for the turbulence simulation has been used to calculate the particle trajectories (Wand and Stock, 1992). The turbulent wind velocity fluctuations (turbulent eddies) (u', v', w') for the three co-ordinate directions, x, y and z (vertical), were generated as a random number from a normal distribution with known standard deviations $(\overline{u'^2})^{1/2}$, $(\overline{v'^2})^{1/2}$ and $(\overline{w'^2})^{1/2}$ (see Section 2.1). For a horizontally homogeneous atmosphere (assumed in this work) the eddy lifetime for the horizontal (downwind, x and crosswind, y) directions was equal. The velocity fluctuations were added to the respective mean wind component to calculate the instantaneous wind. This instantaneous wind persisted for the eddy lifetime and the particles were advected with this velocity. When the eddy lifetime was finished a new velocity fluctuation was generated for the new particle position (independent of the previous one). This procedure is repeated for all the Lagrangian particle in the computational domain. The particle positions during a trajectory simulation was calculated by the following equations (Avila, 1997):

$$x_p = x_{po} + \delta t(\bar{u} + u') \tag{5}$$

$$y_p = y_{po} + \delta t(\bar{v} + v') \tag{6}$$

$$z_p = z_{po} + \delta t(\bar{w} + w') \tag{7}$$

where x_{po}, y_{po} and z_{po} represent the co-ordinates of the initial position of the particles, at start of the time interval δt and $\bar{u}$, $\bar{v}$, $\bar{w}$ are the mean wind velocity components for the three co-ordinate directions x, y, z.

2.3. Concentration calculations

The pollutant concentration as a function of distance from the point of release, may be calculated by various techniques, viz., box counting, residence time method, puff-particle approach, etc. In the box counting and the residence time methods, the whole domain of interest is discritized in control volumes of suitable dimensions and the pollutant concentration is calculated either by

Copyright © 2002 John Wiley & Sons, Ltd.

counting the number of Lagrangian particles in these control volumes (boxes) or from the residence time of the particles in the box. These concentration values are dependent upon the size of the box and in order to have statistically reasonable results these methods require a sufficiently large number of particles to be liberated. If the control volume has dimensions Δx, Δy and Δz and contains N_p number of particles then the concentration $C_{x,y,z}$ at centroid of the box may be calculated using (Hurley, 1994):

$$C_{x,y,z} = \frac{N_p}{\Delta x \Delta y \Delta z} \tag{8}$$

or, using the residence time method which assumes that the concentration is proportional to the residence time of the particles in the box (Reid, 1979). If the number of trajectories simulated is N and t_j is the residence time of the jth trajectory in the box, then the time-integrated concentration is given by

$$C_{x,y,z} = \frac{Q}{N \Delta x \Delta y \Delta z} \sum_{j=1}^{N} t_j \tag{9}$$

where Q is the release source term (#/s) and Δx, Δy and Δz are the box dimensions.

The latter method although yields statistically much better results than the previous one but is very time consuming, again the results are dependent upon the box dimensions.

However, in this work, we have used a puff-particle method (de Haan and Rotach, 1995). Each Lagrangian particle represents the centre of mass of a puff having a Gaussian concentration distribution. The Gaussian distribution had different standard deviation values for the horizontal and vertical directions depending upon the atmospheric stability. According to Hurley (1994) these standard deviations may be obtained from the standard σ curves. The concentration due to a Lagrangian particle was calculated using the equation below and a summation was made over all of the particles in the domain (Yamada and Bunker, 1988).

$$C_{x,y,z} = \frac{1}{(2\pi)^{1.5}} \sum_{p=1}^{N} \frac{1}{\sigma_{x_p} \sigma_{y_p} \sigma_{z_p}} \exp\left(-0.5 \frac{(x_p - x)^2}{\sigma_{x_p}^2}\right) \exp\left(-0.5 \frac{(y_p - y)^2}{\sigma_{y_p}^2}\right) \times \left[\exp\left(-0.5 \frac{(z_p - z)^2}{\sigma_{z_p}^2}\right) + \exp\left(-0.5 \frac{z_p + z^2}{\sigma_{z_p}^2}\right)\right] \tag{10}$$

This scheme yields statistically better results than the simple box counting model and consumes much less time than the residence time method and the results are independent of any box dimensions.

3. NUMERICAL SIMULATION

In the numerical simulation, we use the Lagrangian (Monte Carlo) model in Section 2.2 for the atmospheric dispersion of industrial pollutants. The mean wind field and other turbulent characteristics were assumed to be known in Section 2.1. It was assumed that this wind field

Copyright © 2002 John Wiley & Sons, Ltd.

remained unchanged during the trajectory calculations. The mean wind in the vertical direction (z-axis) was assumed to be zero for a neutral atmosphere.

The turbulence was assumed to be horizontally homogeneous, therefore the velocity fluctuation (turbulent eddy) at a certain height extended over the entire horizontal domain. The particles were assumed to be having the same density as of the atmospheric air (neutral tracers), therefore, the crosstrajectory and the inertial effects did not arise (Avila, 1997). The particle always remained trapped within the eddy with which it once got associated, until the eddy lifetime was over.

Trajectory calculations were performed for about 2000 releases (each containing 100 Lagrangian particles), over a duration of about 1 h. Each Lagrangian particle represented a constant mass of the pollutant released, which was released as a point source but later expanded in dimensions due to the atmospheric turbulence, as a function of the dispersion time/distance. The concentration was calculated by the puff-particle (PP) method which provided the downwind point concentration values independent of any control volume dimensions.

Boundary conditions/Input parameters:

Geostrophic velocity $(u_g) = 17.5\ \mathrm{m\ s^{-1}}$ and $(v_g) = 0$,
$\bar{u}(z \to \infty) = u_g$,
$\bar{v}(z \to \infty) = v_g$,
Atmospheric stability class = D (neutral),
Site latitude $\phi = 40^{\circ}\mathrm{N}$ and
Roughness parameter $z_o = 3$ cm.

4. RESULTS AND DISCUSSION

The numerical simulation results are presented in Figures 6–11. The Lagrangian particle positions in the horizontal and vertical planes are shown in Figures 6(a)–(b), for the release height of 100 m. The plume shapes for other release heights were almost similar (not presented here).

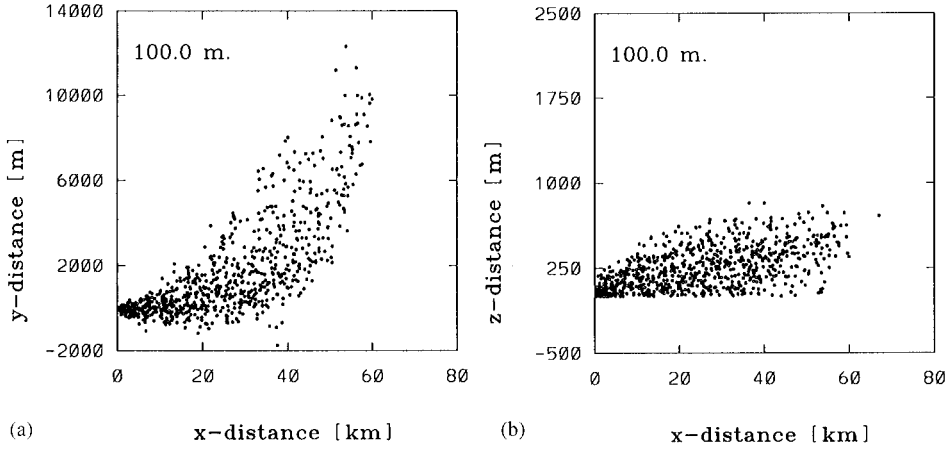

Figure 6. Lagrangian particle positions in (a) horizontal (x–y) and (b) vertical (x–z) planes for the release height of 100 m.

Copyright © 2002 John Wiley & Sons, Ltd.

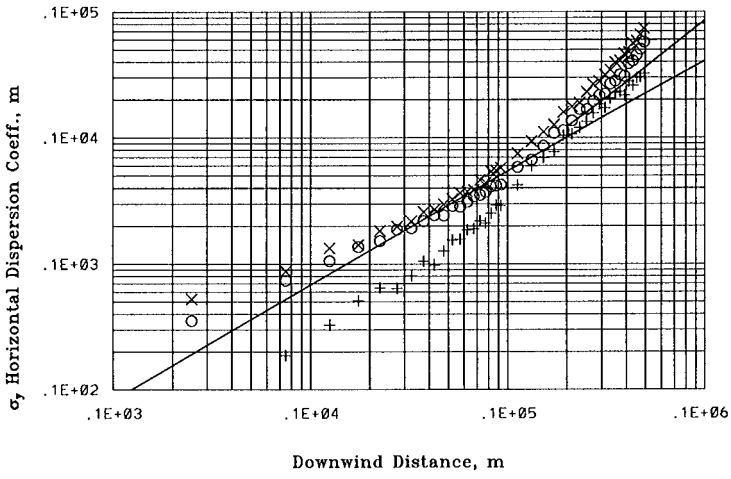

Figure 7. Horizontal dispersion coefficient, continuous line: P–G σ_y (Pasquill, 1976), discrete points: numerical results for release heights of 10, 100 and 500 m (from top to bottom).

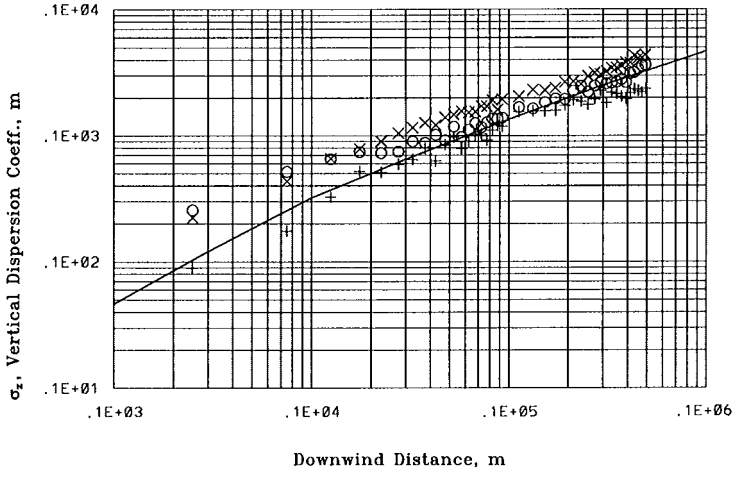

Figure 8. Vertical dispersion coefficient, continuous line: P–G σ_z (Pasquill, 1976), discrete points: numerical results for the release heights of 10, 100 and 500 m (from top to bottom).

The numerically calculated horizontal and vertical dispersion coefficients (σ_y and σ_z) for the release heights of 10, 100 and 500 m, have been compared (see Figures 7 and 8) with the empirical σ's (Pasquill, 1976; Hanna *et al*., 1977). The effect of release height on the dispersion coefficients is clearly observed. Although the reduction in the numerical σ's with increasing release height up to about 100 m is not that pronounced, for enhanced release heights (see that of 500 m), the σ's have relatively much lower values. This behaviour is consistent with the boundary layer theory (Stull, 1988).

The plume spread in the horizontal plane may be seen to be significantly enhanced due to the vertical wind shear for distances exceeding about 10 km (see Figures 6a and 7), where the particle dispersion is not only due to the small turbulent fluctuations but also due to the mean wind

Copyright © 2002 John Wiley & Sons, Ltd.

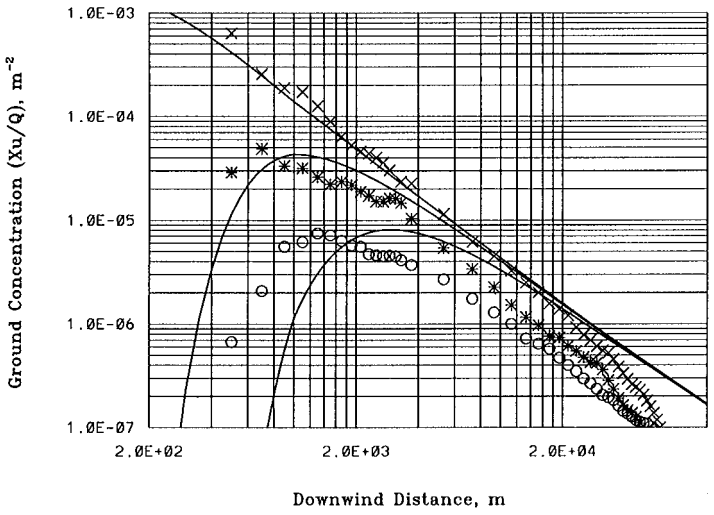

Figure 9. Ground concentration as a function of downwind distance for various release heights; continuous line: GPM, discrete points: numerical results for release heights of 10, 50 and 100 m (from top to bottom).

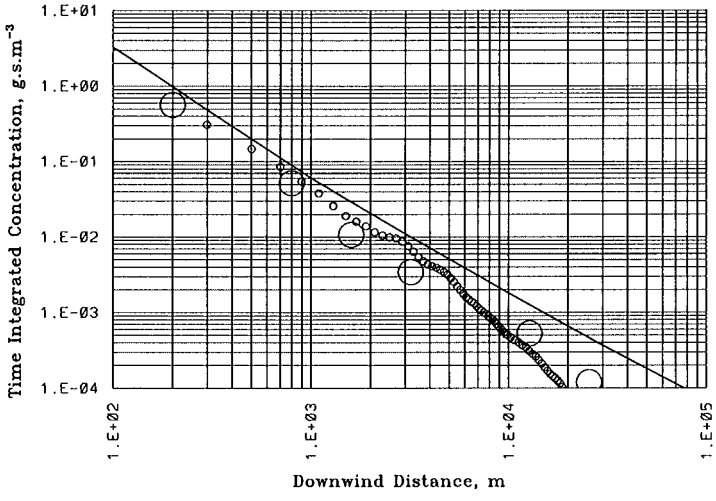

Figure 10. Maximum time integrated ground concentration as a function of downwind distance; small circles: numerical results, big circles: experimental data (run 19).

component in the transverse direction. The numerical dispersion coefficient, however, compared well with the Pasquill's modified σ_y (Pasquill, 1976). The modified σ_y was calculated by adding an empirical factor ($0.03\ x^2\delta\theta^2$) to the square of the previous σ_y (Pasquill, 1976), where $\delta\theta$ (in rad) is the variation in wind direction over the plume depth at the downwind distance x (in m).

The ground concentrations for the release heights of 10, 50 and 100 m, as a function of downwind distance are presented in Figure 9 and compared with the GPM (Turner, 1994). Due to

Copyright © 2002 John Wiley & Sons, Ltd.

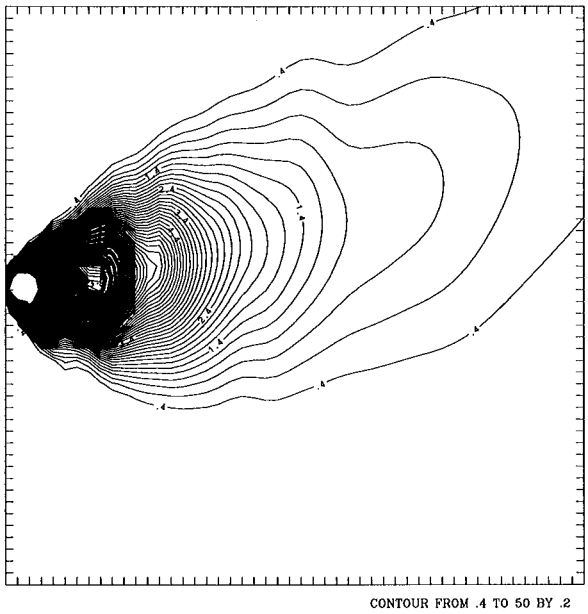

Figure 11. 2D contour map of the numerically calculated time integrated ground concentration ($\times 10^3$ g s m^{-3}) on a horizontal domain of 10×2 km.

the higher plume spread (dispersion coefficients, see Figures 7 and 8) the numerical results were generally below the GPM predictions except for the very near surface release (10 m). The peak concentration predicted by GPM, however, compared well with our numerical results. A comparison of the numerically calculated ground concentration values with the field data are presented in Figure 10. A good comparison of the results is observed with the measurements obtained during the Green Glow experimental run 19 (Fuquay *et al.*, 1964). The measured data correspond to the peak concentration values obtained at arcs of 200, 800, 1600 and 3200 m downwind from the release source. Figure 11 shows a 2D contour map of the numerically calculated concentrations for the same run. A slight shift towards left, in the plume centreline, due to the wind shear may be observed in the 2D contour map. This phenomenon is consistent with the model results obtained by others also (Perdikaris and Mayinger, 1995).

Due to vertical wind shear (induced by associating the co-ordinate system with a rotating earth) the horizontal wind direction changes with height. For a neutral atmosphere an angle of about 26° has been observed, between the surface wind and the geostrophic wind (outside the PBL). This angle is variable with atmospheric stability (about 15° in an unstable and 45° in a stable atmosphere) (Nieuwstadt and van Dop, 1984). As the vertical spread of a plume is increased with the travel distance, a much stronger horizontal mean wind component is felt by the plume and this results in an enhanced σ_y. It is therefore necessary to use modified dispersion coefficients in the GPM, for distances exceeding about 10 km, or as an alternative, a 3D mathematical model (as our Lagrangian model) should be used.

Copyright © 2002 John Wiley & Sons, Ltd.

5. CONCLUSIONS

The Lagrangian Monte Carlo particle dispersion models work very efficiently for the atmospheric dispersion of effluents. Although we in these calculations assumed a perfect ground reflection during the trajectory calculations, however, any other criterion for ground reflection may easily be incorporated. As the particle model is always coupled with a wind field model, the complex terrain and meteorological conditions are inherently taken into account.

In order to incorporate the effect of vertical wind shear the modified dispersion coefficient (σ_y) should be used with the Gaussian plume model. As an alternative, a much reliable 3D numerical model as presented here, may be used at a slightly higher computational cost. Such a numerical model may also be used in a complex topography region with mountains, where the conventional Gaussian models are not suitable.

ACKNOWLEDGEMENTS

The authors acknowledge the support of the Visualization Laboratory (DGSCA-UNAM) Mexico. The numerical calculations of this paper were performed using the CRAY-Y-MP and Silicon Graphics Origen 2000 computers of the 'Universidad Nacional Autónoma de México', 'Instituto Mexicano del Petróleo' and 'Instituto Nacional de Investigaciones Nucleares'. This investigation was supported by the 'Consejo Nacional de Ciencia y Tecnología' through the project 3328P-A, and the 'Dirección General de Apoyo al Personal Académico-UNAM', through the project PAPITT No. IN105798.

REFERENCES

Avila R. 1997. Simulación Numérica de la Dispersión de una Nube de Partículas Sólidas Liberada a la Atmósfera. *Tesis de Doctorado*, División de Estudios de Posgrado Facultad de Ingeniería, U.N.A.M.

Davis PA. 1983. Markov chain simulation of vertical dispersion from elevated sources into the neutral planetary boundary layer. *Boundary Layer Meteorology* **26**:355–376.

de Haan P, Rotach MW. 1995. A puff-particle dispersion model. *International Journal of Environment and Pollution* **5**:350–359.

Fuquay JJ, Simpson CL, Hinds WT. 1964. Prediction of environmental exposures from sources near the ground based on Hanford experimental data. *Journal of Applied Meteorology* **3**:761–770.

Hanna SR. 1982. *Applications in Air Pollution Modeling in Atmospheric Turbulence and Air Pollution Modeling*, Nieuwstadt FTM, van Dop H (eds). D. Reidel: Dordrecht.

Hanna SR, Briggs GA, Deardorff J, Egan BA, Gifford FA, Pasquill F. 1977. AMS workshop on stability classification schemes and sigma curves—summary of recommendations. *Bulletin of the American Meteorological Society* **58**(12):1305–1309.

Haugen DA. 1959. Project Prairie Grass: a field program in diffusion. Geophysical Research Papers, No. 59, vol. III, *Technical Report* AFCRC-TR-58-235, Air Force Cambridge Research Center, Cambridge.

Hurley P. 1994. PARTPUFF—a Lagrangian particle-puff approach for plume dispersion modeling applications. *Journal of Applied Meteorology* **33**:285–294.

Lettau HH. 1962. Theoretical wind spirals in the boundary layer of a barotropic atmosphere. *Beiträge zur Physik der Atmosphäre* **35**:195–212.

Miller CW, Hively LM. 1987. A review of validation studies for the Gaussian plume atmospheric dispersion model. *Nuclear Safety* **28**(4):522–531.

Nieuwstadt FTM, van Dop H. 1982. *Atmospheric Turbulence and Air Pollution Modeling*. D. Reidel: Dordrecht.

Pasquill F. 1976. Dispersion parameters in Gaussian plume modeling. *Technical Report* EPA-600/4-76-030b, Environmental Protection Agency, Washington, D.C.

Perdikaris GA, Mayinger F. 1995. Numerical simulation of the spreading of buouyant gases over topographically complex terrain. *International Journal of Energy Research* **19**:51–61.

Reid JD. 1979. Markov chain simulation of vertical dispersion in the neutral surface layer for surface and elevated releases. *Boundary Layer Meteorology* **16**:3–22.

Copyright © 2002 John Wiley & Sons, Ltd.

Stull R. 1988. *An Introduction to the Boundary Layer Meteorology*. Kluwer: Boston.
Turner DB. 1994. *Workbook of Atmospheric Dispersion Estimates*: *An Introduction to Dispersion Modeling*. Lewis Publishers, Boca Raton, Florida.
Turner DB. 1997. The long lifetime of the dispersion methods of Pasquill in US regulatory air modeling. *Journal of Applied Meteorology* **36**:1016–1020.
Wang LP, Stock DE. 1992. Stochastic trajectory models for turbulent diffusion: Monte Carlo process versus Markov chains. *Atmospheric Environment* **26A**(9):1599–1607.
Yamada T, Bunker S. 1988. Development of a nested grid, second moment turbulence closure model and application to the 1982 ASCOT brush creek data simulation. *Journal of Applied Meteorology* **27**:562–578.

Copyright © 2002 John Wiley & Sons, Ltd.